

# Semantics-Aware Communication: A Differentiated Allocation Perspective

Fangming Zhao, Nikolaos Pappas, and Howard H. Yang

**Abstract**—We study the joint optimization of timeliness and reliability in semantics-aware Wireless Networked Control Systems (WNCS) under computation resource constraints. The sampled data are categorized into regular and critical tasks based on the semantic states, facilitating differentiated resource allocation. Task-aware Age of Actuation (AoA) and Cost of Missing Actuation (CoMA), are used to characterize the task-level freshness and the reliability penalty of missed actuations, respectively. By modeling the controller as a discrete-time multi-rate Geo/D/C/C queue, we evaluate the performance of regular and critical tasks, the latter imposing higher computational demands. Results confirm that differentiated resource allocation across heterogeneous tasks effectively guarantees the actuation reliability of critical tasks in severely constrained environments.

**Index Terms**—Semantics-aware, multiple server queueing, Age of Actuation (AoA), CoMA.

## I. INTRODUCTION

The Age of Information (AoI) serves as a fundamental metric to quantify information freshness in time-critical networks [1], [2]. By capturing the time elapsed since the generation of the most recently received update, AoI facilitates the design of communication systems with timeliness constraints [3]. However, AoI remains a transmission-centric metric that falls short in WNCS. In such systems, the intrinsic utility of data depends heavily on actuation rather than mere packet delivery. Recognizing that system efficacy is governed by task semantics, it is imperative to shift the focus toward semantics-aware communication [4]. Under this paradigm, transmission timing and resource allocation are explicitly designed to meet the underlying execution objectives of the receiver.

Within this transmission-to-execution framework, the AoA metric characterizes the temporal mismatch between the current system state and the most recently executed control action [5]. By shifting the focus from information reception to action execution, AoA provides a direct link between communication timeliness and control effectiveness. Prior studies on AoA are largely limited to single-stream settings, overlooking the heterogeneity of different tasks. In real-time control, dropping a critical packet can severely degrade system stability, necessitating differentiated treatment in system design. Therefore, we need to evaluate the AoA for each different class independently, which is referred to as task-aware AoA.

Furthermore, for rare yet highly critical events, AoA alone is insufficient to characterize their true impact, as the low sampling/generation probability of such events dominates their performance evaluation. This observation motivates the CoMA metric. As a weighted extension of the conventional packet

drop rate, CoMA explicitly reflects the heterogeneous importance of different information streams. By combining the AoA of each task and CoMA for execution reliability, we can capture the multidimensional requirements of WNCS via Pareto optimization [6].

Despite recent advancements in semantics-aware estimation [4] and scheduling [7], most existing works primarily emphasize communication resource allocation while overlooking the joint effects of communication and computation. In systems constrained by limited processing capacity, the implicit interaction between execution reliability and competition for computing resources remains underexplored. To solve these issues, we develop a framework that jointly models: (i) task-oriented sample transmission over imperfect uplinks; (ii) the dynamic allocation and release of computational resources at the controller; (iii) heterogeneous resource requirements of different task types. The main contributions of this work are summarized as follows.

- We model a semantics-aware WNCS constrained by limited computational resources. Specifically, a multi-rate Geo/D/C/C queueing system is developed to capture the computational resource dynamics at the controller. We compare its blocking probability against both the Geo-/Geo/C/C model and the continuous-time Erlang formula. The results reveal that the blocking probability in discrete-time loss queueing systems is not strictly insensitive to the service distribution. Nevertheless, a stochastic service model can still be employed as an upper-bound approximation for deterministic service, thereby mitigating the curse of dimensionality caused by multi-rate deterministic service models.
- We analyze two semantics-aware metrics: Task-aware AoA and CoMA, which reflect the timeliness and reliability of task execution. The results reveal that under limited resources, heterogeneous task flows can exhibit strong competition, where executing one task type affects the timeliness of others, and differentiated resource allocation across heterogeneous tasks effectively optimizes resource efficiency in severely constrained environments.

## II. SYSTEM MODEL

We consider a WNCS that integrates communication and computation. As illustrated in Fig. 1, the system comprises multiple modules: a sensor to generate sampled data, an uplink channel for data transmission, an edge controller to process tasks and make decisions, and an actuator to execute the commands. In the following, we introduce the mathematical

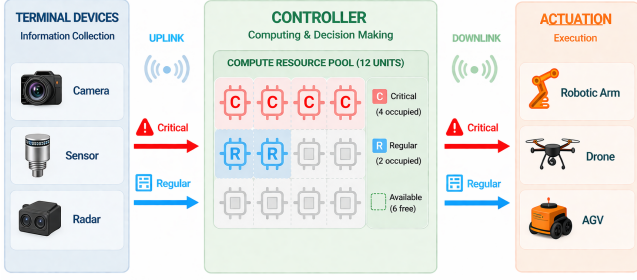


Fig. 1. Semantics-aware wireless networked control systems.

modeling of each module, which allows for formulating the performance metrics: the task-aware AoA and the CoMA.

#### A. Wireless Networked Control System Modeling

1) **Semantics-Aware Information Generation:** We consider a discrete-time framework where the sensor generates sampling data to support distinct perception and control functionalities. To optimize the utilization of wireless resources while guaranteeing system stability, the generated data is classified into two categories: regular information and critical information. We aim to implement differentiated resource allocation based on the semantics of the information.

Specifically, the semantic value of the data is dynamically evaluated based on the local physical state. A regular packet is generated when the discrepancy exceeds a predefined regular threshold but remains within a safe margin. In contrast, a critical packet is triggered when the discrepancy violates a critical safety limit. Let  $g_1$  and  $g_2$  denote the overall probabilities of generating regular information and critical information in a given time slot, respectively, where  $g_1 + g_2 \leq 1$ . The remaining probability  $1 - g_1 - g_2$  accounts for the idle time slots where the physical state is well-predicted and no data is generated. To streamline the presentation, we refer to the control commands corresponding to the regular and critical information streams as Task 1 and Task 2, respectively.

2) **Uplink Communication Model:** Once a packet is generated, the sensor attempts to transmit it to the controller over the uplink wireless channel. The admission probability is  $\eta_1$  when attempting to transmit the data of Task 1, and  $\eta_2$  when attempting to transmit the data of Task 2. The uplink channel experiences small-scale fading, where the fading envelope  $|h_u|$  follows a Nakagami- $m$  distribution with a shape parameter  $m$  and a normalized average power  $\mathbb{E}[|h_u|^2] = 1$ . Additionally, it suffers from large-scale path loss modeled as  $d_u^{-\alpha_u}$ , where  $d_u$  is the distance from the sensor to the controller and  $\alpha_u$  is the path-loss exponent. Consequently, the received signal-to-noise ratio (SNR)  $\gamma_{u,i}$  at the controller is  $\gamma_{u,i} = \frac{P_{T,i}|h_u|^2 d_u^{-\alpha_u}}{\sigma^2}$ , where  $P_{T,i}$  is the transmit power of the sensor, and  $\sigma^2$  is the noise power at the controller. If  $\gamma_{u,i}$  falls below a decoding threshold  $\bar{\gamma}$ , the uplink packet is lost. The uplink transmission success probability for task  $i$ , denoted by  $p_{u,i}$ , is given by  $p_{u,i} = \mathbb{P}(\gamma_{u,i} \geq \bar{\gamma})$ .

However, combating channel impairments to guarantee the required  $p_{u,i}$  requires sufficient transmit power  $P_{T,i}$ , which

inherently drains the limited battery life of the sensor. To ensure the practical feasibility of the proposed strategy, we investigate a time horizon  $T$  bounded by a finite total energy capacity  $E$ . Consequently, the differentiated power allocation among heterogeneous tasks must be strictly constrained such that the long-term energy consumption does not exceed  $E$ .

3) **Controller with Limited Computation Resource:** The controller acts as a computing node with limited computational capacity, comprising  $C$  parallel and independent computation units. Upon successfully decoding an uplink packet, the receiver performs a lightweight header parsing to identify its semantic type (Task 1 or Task 2). Based on this identification, the controller allocates the computation resource following a semantics-aware resource allocation policy<sup>1</sup>:

- **Task 1:** requiring  $N_1 = 1$  computation unit. The deterministic service time is  $D_{C,1}$  slots.
- **Task 2:** requiring  $N_2 = N$  computation units ( $N > 1$ ) for complex calculations. The assigned  $N$  units process the task in a synchronous parallel manner, with a deterministic service time of  $D_{C,2}$  slots.

All computation units are non-preemptive. Once allocated to a task, they remain occupied until the computation is completed. If computational resources are insufficient upon task arrival or the task is rejected by the controller's admission policy, the task is discarded without entering the buffer. Therefore, the dynamic of the computational resource pool can be modeled as a multi-rate Geo/D/C/C queueing system.

4) **Downlink Communication:** The traffic link of actuation commands from the controller to the actuator is assumed to be error-free, and only considers constant delay  $D_{T,i}$ . This assumption is well justified by the highly asymmetric nature of WNCs links: the controller typically operates with an ample power budget and a continuous energy supply, enabling it to employ advanced channel-adaptive schemes to guarantee a near-100% successful delivery rate. Consequently, the primary system bottlenecks are dominated by the uplink transmission and the computation queueing.

5) **Actuation Model:** The actuation system is deployed at the end device. Successfully processed task commands are immediately executed. If a task is dropped due to uplink transmission failure or computational resource limits, the actuator maintains the last valid command<sup>2</sup>. While ensuring continuous physical input, holding stale commands degrades system stability. This directly motivates our use of the AoA and the CoMA to quantify the penalty of state deviations.

<sup>1</sup>We differentiate resource allocation as follows: regular tasks use semantic priors for efficient recovery, while critical tasks require high-fidelity reconstruction, thereby requiring greater computational effort.

<sup>2</sup>Our differentiated allocation strategy exploits the disparate error tolerances inherent in semantics-aware control systems. While packet loss in critical tasks causes catastrophic failure, regular tasks possess semantic redundancy. Leveraging Zero-Order Hold mechanisms [4] at the actuator, the system exhibits graceful degradation against the dropping of regular tasks. This property fully justifies sacrificing regular tasks to guarantee the ultra-reliability of critical tasks.

## B. Performance Metrics

In time-critical systems, the AoI metric is commonly adopted as a key performance metric to quantify information freshness. The AoI is defined as the time elapsed since the generation of the most recently successfully received data packet. According to the original definition, the AoI metric does not differentiate between the nature of data flows and focuses solely on the transmission process from source to destination. As such, it does not adequately capture the heterogeneity and computation execution processes inherent in task-oriented networks.

In this work, we further extend two performance metrics: the AoA and the CoMA [5]. Given the presence of different types of tasks, we evaluate these metrics separately for each task to capture their distinct characteristics and their impact on performance. The definition given as follows:

**Definition 1.** (*Task-aware Age of Actuation*) Consider a real-time communication system that involves  $n$  types of tasks command, task  $i$ ,  $i \in \{1, 2, \dots, n\}$ . Let  $A_i(t_j)$ ,  $j \geq 1$  be the sequence of generation times of information packets belonging to task type  $i$  that were successfully executed by the receiver. Let  $t_j$  denote the corresponding times at which these execution events occur. Among the successfully executed packets of task type  $i$  until time  $t$ , denote by

$$n_i(t) = \arg \max_j \{A_i(t_{n_i(t)}) | t_j \leq t\}. \quad (1)$$

Therefore, the AoA for task type  $i$  at time  $t$  is defined as

$$\Delta_i(t) = t - A_i(t). \quad (2)$$

That is,  $A_i(t)$  represents the time elapsed since the generation of the most recently executed packet of task type  $i$ . The AoA is dropped exclusively upon the successful execution of a packet belonging to the same task stream.

Follow the definition, the time-average function of the AoA metric (i.e., time-average AoA) is given by

$$\bar{\Delta}_i(t) = \lim_{T \rightarrow \infty} \frac{1}{T} \mathbb{E} \left[ \sum_{t=1}^T \Delta_i(t) \right]. \quad (3)$$

The time-average AoA characterizes the long-term timeliness of operator actuation. Moreover, to evaluate the reliability of transmission over imperfect channels and the performance degradation caused by insufficient computational resources. We extend the general penalty-based performance metric, the Cost of Missing Actuation, to the multi-task case to denote the cost of discarding a task command. Specifically, a penalty of  $\omega_i$  is incurred for each unsuccessfully executed Task  $i$ .

**Definition 2.** *Cost of Missing Actuation (CoMA):* the average cost of a discarded command during the operator period, as a result of insufficient resources.

$$C_{\text{MA}} = \lim_{T \rightarrow \infty} \frac{1}{T} \sum_{t=0}^T \sum_{i \in \mathcal{T}} L_i(t) \mathbb{I}_i(t), \quad (4)$$

where  $\mathbb{I}_i(t) \in \{0, 1\}$  is an indicator function, and  $\mathbb{I}_i(t) = 1$  indicates the class  $i$  task loss or attempts to execute but fails

due to insufficient resources.  $L_i(t)$  denote the cost associated with the failure of a class  $i$  task at time  $t$ .

Unlike the packet loss rate, which merely counts lost data equally, CoMA quantifies the impact of missing information on task execution. Its key function is to enable the system to safeguard mission-critical packets while discarding redundant ones at an early stage, thereby maximizing resource efficiency.

## III. PERFORMANCE ANALYSIS

This section provides a detailed analysis of the proposed performance metrics. By leveraging a discrete-time graphical approach [8], the time-average AoA for task  $i$ , denoted by  $\Delta_i$ , can be formulated as

$$\Delta_i = \frac{\mathbb{E}[X_i^2] + \mathbb{E}[X_i]}{2\mathbb{E}[X_i]} + \mathbb{E}[D_{C,i}] + \mathbb{E}[D_{T,i}], \quad (5)$$

where random variable  $X_i$  represents the time interval between two consecutive executions of task  $i$ . The analytical expressions for these metrics are established in Theorem 1.

**Theorem 1.** *The time-average AoA of task  $i$  can be expressed as*

$$\bar{\Delta}_i = \frac{1}{g_i \eta_i p_{u,i} \mathbb{P}(\Gamma \geq N_i)} + D_{C,i} + D_{T,i}. \quad (6)$$

The CoMA can be given by

$$C_{\text{MA}} = \sum_{i \in \{1,2\}} \omega_i g_i (1 - \eta_i p_{u,i} \mathbb{P}(\Gamma \geq N_i)), \quad (7)$$

where  $p_{u,i} = \frac{\int_0^\infty \psi_i t^{m-1} e^{-t} dt}{\int_0^\infty t^{m-1} e^{-t} dt}$ , and  $\psi_i = \frac{\bar{\gamma} \sigma^2 d_u^\alpha}{P_{T,i}}$ .

*Proof:* Due to limited space, we only provide a sketch here. First, using the property of Bernoulli processes, we can obtain the first and second moments of the  $X_i$ . The  $\bar{\Delta}_i$  is derived by applying these moments and constant service and transmission delay to (5). Second, the CoMA is formulated by evaluating the joint probability of successful admission, uplink transmission, and sufficient computation, scaled by task penalties  $\omega_i$ . Finally, the transmission probability  $p_{u,i} = \mathbb{P}(\gamma_{u,i} \geq \bar{\gamma})$  is reformulated as  $\mathbb{P}(|h_u|^2 \geq \psi_i)$ , which is then solved via a variable substitution of the Gamma distribution. ■

**Remark 1.** *As a baseline for comparison, the time-average AoI from the sensor to the controller can be expressed as*

$$\bar{\Delta} = \frac{1}{g_1 \eta_1 p_{u,1} + g_2 \eta_2 p_{u,2}}. \quad (8)$$

From (6)–(7), we observe that the performance of different task flows is coupled through the probability of sufficient computational resources. Specifically, the task 1 admission probability,  $\eta_1$ , influences resource occupancy, which in turn affects resource availability and timeliness for task 2. Therefore, in resource-constrained regimes, the differentiated treatment of heterogeneous semantic streams is crucial to maximizing the overall system efficacy.

Furthermore, calculating these metrics requires deriving the probability that the controller possesses sufficient computa-

tional units upon the arrival of Task  $i$ ,  $\mathbb{P}(\Gamma \geq N_i)$ . We then model the computation resource allocation and release.

### A. Computation Resource Dynamic in Deterministic Service

The allocation and release of computation units give rise to system dynamics. When the computation service time is deterministic, the memoryless property of task departure is strictly broken. To capture the remaining processing time of each active task, we model the system evolution using a  $(D_1 + D_2)$ -dimensional discrete-time Markov chain (DTMC).

Let  $\mathbf{v}_i = [v_{i,1}, v_{i,2}, \dots, v_{i,D_i}]^T \in \{0, 1\}^{D_i}$  denote the execution pipeline for Task  $i \in \{1, 2\}$ , where  $D_i$  is the deterministic required service time (in slots). The binary element  $v_{i,k} = 1$  indicates that there is currently a Task  $i$  instance with exactly  $k$  slots of remaining execution time, and  $v_{i,k} = 0$  otherwise. The system state is then defined as a composite vector  $\mathbf{s} = (\mathbf{v}_1, \mathbf{v}_2)$ . The number of currently active tasks of type  $i$ , denoted by  $n_i(\mathbf{v}_i)$ , is  $\ell_1$ -norm of the vector, i.e.,  $n_i(\mathbf{v}_i) = \|\mathbf{v}_i\|_1 = \sum_{k=1}^{D_i} v_{i,k}$ . Consequently, the valid state space under the capacity constraint is given by:  $\Omega_{\text{det}} = \{(\mathbf{v}_1, \mathbf{v}_2) \in \{0, 1\}^{D_1} \times \{0, 1\}^{D_2} \mid \|\mathbf{v}_1\|_1 + N\|\mathbf{v}_2\|_1 \leq C\}$ .

The exact number of feasible states can be derived as:

$$|\mathcal{S}| = \sum_{n_2=0}^{\min(D_2, \lfloor C/N \rfloor)} \sum_{n_1=0}^{\min(D_1, C - Nn_2)} \binom{D_1}{n_1} \binom{D_2}{n_2}, \quad (9)$$

where the binomial coefficient  $\binom{D_i}{n_i}$  represents the number of possible execution that contain exactly  $n_i$  active tasks.

The state transition is driven by the deterministic aging of existing tasks and the admission of newly arrived tasks. Let  $a_i(t) \in \{0, 1\}$  be the admission indicator for Task  $i$  at time slot  $t$ , respectively. As time progresses from slot  $t$  to  $t + 1$ , all active tasks advance one step towards completion. A task with  $v_{i,1}(t) = 1$  completes its execution and departs the system, releasing its resources. Simultaneously, a newly admitted task enters the pipeline with a full remaining time of  $D_i$ . Mathematically, this physical evolution is modeled as a deterministic shift operation  $\mathcal{F}(\mathbf{v}_i, a_i)$ :

$$v_{i,k}(t+1) = \begin{cases} v_{i,k+1}(t), & \text{for } 1 \leq k \leq D_i - 1, \\ a_i(t), & \text{for } k = D_i. \end{cases} \quad (10)$$

The admission probabilities  $P_{\mathcal{A}}(a_1, a_2 \mid \mathbf{s})$  follow the same logic as the memoryless case, heavily depending on the current available capacity  $C - \|\mathbf{v}_1\|_1 - N\|\mathbf{v}_2\|_1$ . Let  $\mathcal{A} = \{(0, 0), (1, 0), (0, 1)\}$  denote the feasible admission action space. The state transition probability  $P_{\mathcal{S}}^{\mathbf{s}'}$  from current state  $\mathbf{s} = (\mathbf{v}_1, \mathbf{v}_2)$  to the next state  $\mathbf{s}' = (\mathbf{v}'_1, \mathbf{v}'_2)$  is concisely expressed as:

$$\sum_{(a_1, a_2) \in \mathcal{A}} P_{\mathcal{A}}(a_1, a_2 \mid \mathbf{s}) \mathbb{I}(\mathbf{v}'_1 = \mathcal{F}(\mathbf{v}_1, a_1)) \mathbb{I}(\mathbf{v}'_2 = \mathcal{F}(\mathbf{v}_2, a_2)), \quad (11)$$

where the indicator function  $\mathbb{I}(\cdot)$  ensures that the transition probability is strictly zero unless the target state exactly

matches the deterministic shift execution pipeline, and:

$$P_{\mathcal{A}}(a_1, a_2 \mid \mathbf{s}) = \begin{cases} g_1 \eta_1 p_{u,1} \mathbb{I}(n_1(\mathbf{s}) + Nn_2(\mathbf{s}) + 1 \leq C), & \text{if } (a_1, a_2) = (1, 0), \\ g_2 \eta_2 p_{u,2} \mathbb{I}(n_1(\mathbf{s}) + Nn_2(\mathbf{s}) + N \leq C), & \text{if } (a_1, a_2) = (0, 1), \\ 1 - P_{\mathcal{A}}(1, 0 \mid \mathbf{s}) - P_{\mathcal{A}}(0, 1 \mid \mathbf{s}), & \text{if } (a_1, a_2) = (0, 0). \end{cases}$$

Next, we solve for the steady-state probability vector  $\mathcal{S}$ . To achieve this, we traverse the state transition space via Breadth-First Search (BFS) without exhaustive enumeration, and subsequently solve the global balance equation  $\mathcal{S}(\mathbf{P} - \mathbf{I}) = \mathbf{0}$  subject to the normalization constraint  $\mathcal{S}\mathbf{1} = 1$ . However, it is evident from (9) that the size of the state space increases exponentially with both the total amount of computational resources and the computation delay of each task. As a result, exact numerical evaluations that require constructing the full steady-state transition matrix and employing sparse matrix solvers remain computationally tractable only at limited scales, such as  $C = 20$  and  $D_{C,i} = 10$ .

Alternatively, by approximating the deterministic service completions as a Bernoulli arrival process, the resource release process leverages the memoryless property. This allows us to bypass tracking execution-time states, successfully reducing the DTMC from  $(D_1 + D_2)$  dimensions to a strictly 2-dimensional model, which is presented in the next subsection.

### B. Computation Resource Dynamic in Random Service

When the computation service time follows a geometric distribution, the resource pool can be modeled as a multi-rate Geo/Geo/C/C queueing. We can model this process as a two-dimensional DTMC. The state is defined as  $\mathbf{s} = (n_1, n_2)$ , representing the number of active Task 1 and Task 2 instances, respectively. Let  $\Omega_{\text{Geo}}$  be the state space of the Markov chain, given by  $\Omega_{\text{Geo}} = \{(n_1, n_2) \mid n_1, n_2 \in \mathbb{N}_+, n_1 + Nn_2 \leq C\}$ . The total number of valid states, denoted by  $|\mathcal{S}|$ , is:

$$|\mathcal{S}| = \frac{1}{2} (C + 1 + (C + 1 - N \times \lfloor \frac{C}{N} \rfloor)) (\lfloor \frac{C}{N} \rfloor + 1) \approx \frac{C^2}{2N}. \quad (12)$$

The state transition from current state  $(n_1, n_2)$  to the next state  $(\nu, \varphi)$  depends on two independent sub-processes in a single time slot: (i) the departure of completed tasks, and (ii) the admission of newly arrived tasks based on available resources. First, we define the probability mass function of the number of remaining tasks. Since each task independently completes with probability  $\mu_i = 1/D_{C,i}$ , the number of remaining Task  $i$  instances, denoted by  $\kappa$ , follows a Binomial distribution  $B(n_i, 1 - \mu_i)$ . We define this departure function as:

$$B(n_i, \mu_i \mid \kappa) = \begin{cases} \binom{n_i}{\kappa} (1 - \mu_i)^\kappa \mu_i^{n_i - \kappa}, & 0 \leq \kappa \leq n_i, \\ 0, & \text{otherwise.} \end{cases} \quad (13)$$

Second, we define the task admission probabilities. A newly arrived task is admitted only if the system has sufficient remaining capacity. Let  $a_1 \in \{0, 1\}$  and  $a_2 \in \{0, 1\}$  denote the number of admitted Task 1 and Task 2 instances, respectively.

Given the current state  $(n_1, n_2)$ , the joint admission probability  $P_A(a_1, a_2 | n_1, n_2)$  is defined as:

$$\begin{cases} P_A(1, 0 | n_1, n_2) = g_1 \eta_1 p_{u,1} \cdot \mathbb{I}(n_1 + N n_2 + 1 \leq C) \\ P_A(0, 1 | n_1, n_2) = g_2 \eta_2 p_{u,2} \cdot \mathbb{I}(n_1 + N n_2 + N \leq C) \\ P_A(0, 0 | n_1, n_2) = 1 - P_A(1, 0 | n_1, n_2) - P_A(0, 1 | n_1, n_2), \end{cases}$$

where  $\mathbb{I}(\cdot)$  is the indicator function that returns 1 if the condition is true, and 0 otherwise. Finally, the target next state  $(\nu, \varphi)$  is simply the sum of the remaining tasks and the newly admitted tasks. By applying the law of total probability over all possible admission events, the unified state transition probability  $P_{(n_1, n_2)}^{(\nu, \varphi)}$  is concisely expressed as:

$$\sum_{(a_1, a_2) \in \mathcal{A}} P_A(a_1, a_2 | n_1, n_2) B(n_1, \mu_1 | \nu - a_1) B(n_2, \mu_2 | \varphi - a_2). \quad (14)$$

The state transition probability matrix is denoted by  $\mathbf{P} \triangleq [P_{(n_1, n_2)}^{(\nu, \varphi)}] \in \mathbb{R}^{|\mathcal{S}| \times |\mathcal{S}|}$ . Leveraging the structural properties of the proposed DTMC's transition matrix, we can efficiently solve the system by employing a matrix-geometric approach. Detailed derivations are provided in Appendix A.

Further, we also present the steady state probability results for the continuous-time M/G/C/C model, which often use as an approximation to the discrete time queueing.

**Approximation:** (Erlang's loss formula) The steady-state distribution of the number of tasks in the system for an M/G/C/C model is given by [9]:

$$S_{n_1, n_2} = \frac{\frac{\rho_1^{n_1} \rho_2^{n_2}}{n_1! n_2!}}{\sum_{(n_1, n_2) \in \Omega} \frac{\rho_1^{n_1} \rho_2^{n_2}}{n_1! n_2!}}, \quad \rho_i = \frac{g_i \eta_i p_{u,i}}{\mu_i}, \quad i \in \{1, 2\}. \quad (15)$$

This result can be used as a tight approximation under light traffic, the system dynamics are largely governed by transitions between adjacent states, with multi-server transitions for different task occurring with negligible probability. Consequently, Erlang's loss formula provides a tractable approximation for characterizing system behavior, albeit at the expense of analytical accuracy.

Based on the steady-state distribution analysis, the probability that task  $i$  is successfully allocated a sufficient computation unit can be obtained as:

$$\mathbb{P}(\Gamma \geq N_i) = \sum_{s \in \Omega} S(s) \cdot \mathbb{I}(n_1(s) + N n_2(s) + N_i \leq C). \quad (16)$$

Fig. 2 compares the blocking probabilities when task  $i$  arrives at the controller, i.e.,  $1 - \mathbb{P}(\Gamma \geq N_i)$ , for the Geo/D/C/C, Geo/Geo/C/C, and M/G/C/C queues, all modeled under identical traffic loads. The exact Geo/D/C/C analysis closely matches the simulations when the state space is moderate in size. Notably, the Geo/D/C/C queue exhibits the lowest blocking probability, as deterministic service times eliminate departure variance. Consequently, the Geo/Geo/C/C and M/G/C/C models serve as valid analytical upper bounds, with negligible approximation gaps in the light-traffic regime. Crucially, the Geo/Geo/C/C queue model provides a tight surrogate for eval-

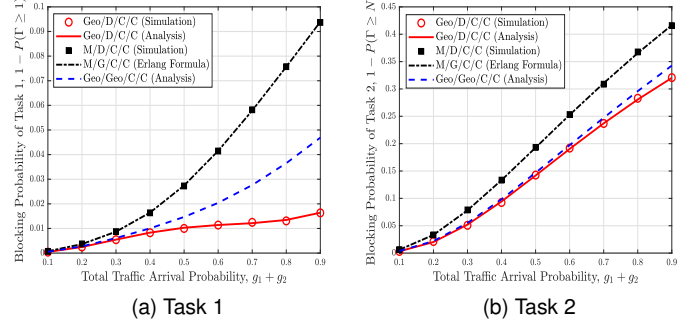


Fig. 2. Queueing model comparison.  $C = 12$ ,  $N = 4$ ,  $D_{C,1} = 5$ ,  $D_{C,2} = 10$ ,  $\eta_1 = \eta_2 = 1$ ,  $p_{u,i} = 1$ ,  $g_1/g_2 = 4$ .

uating the performance of critical Task 2, effectively bypassing the curse of dimensionality inherent in the exact multi-task Geo/D/C/C analysis.

### C. Optimization Problem Formulation

In the considered WNCS, the ultimate goals are to optimize CoMA caused by data drops and the timeliness of the regular task streams. Thus, we formulate the following bi-objective optimization problem:

$$\mathcal{P}1 : \text{minimize}_{P_{T,1}, P_{T,2}, \eta_1, \eta_2} \{ \mathcal{C}_{MA}, \bar{\Delta}_1 \}, \quad (17)$$

$$\text{subject to } g_1 \eta_1 P_{T,1} + g_2 \eta_2 P_{T,2} \leq E/T, \quad (18)$$

$$\eta_1, \eta_2 \in (0, 1], P_{T,1}, P_{T,2} > 0. \quad (19)$$

The constraint (18) accounts for the total power consumption constraint of the system, and constraint (19) is the physical constraints of the parameters.

Without resorting to algorithmic simplifications of the optimization problem, we use a search method to verify whether applying a differentiated strategy to heterogeneous semantic data can provide performance improvements for the entire system, as discussed in the next section.

## IV. NUMERICAL RESULTS AND DISCUSSIONS

In this section, we validate the theoretical analysis through simulations and discuss the impact of various parameters on the time-average AoA of each task, and the CoMA. Unless explicitly stated, we assume  $C = 8$ ,  $N = 4$ ,  $\omega_1 = 1$ ,  $\omega_2 = 10$ ,  $g_1 = 0.4$ ,  $g_2 = 0.1$ ,  $D_{C,i} = 10$  slot,  $D_{T,i} = 0.1$  slot,  $\sigma^2 = -80$ dB,  $\bar{\gamma} = 5$ dB,  $m = 1$ ,  $\alpha_u = 3$ ,  $d_u = 50$ ,  $E/T = 0.18$  W, simulation time is  $10^6$  slot.

Fig. 3 illustrates the performance metrics versus admission probability of task 1  $\eta_1$ . Increasing  $\eta_1$  degrades AoA of task 2 and CoMA. The task-level performance analysis clearly reveals the resource contention among heterogeneous data flows. This confirms that task-specific metrics provide a more accurate characterization of the system than aggregated AoI. Furthermore, we observe that approximating deterministic service with a stochastic service yields a tight fit in the loss system. Additionally, integrating the Erlang loss formula into our analytical expression provides an upper bound on system performance evaluation.

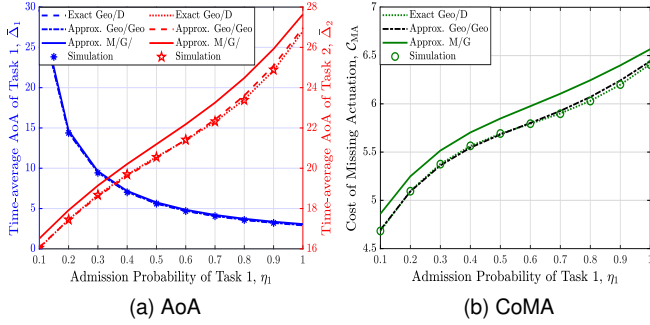


Fig. 3. Performance metric versus actuation probability of task 1.  $P_{T,1} = 0.05 W$ ,  $P_{T,2} = 0.2 W$ ,  $\eta_2 = 0.8$ .

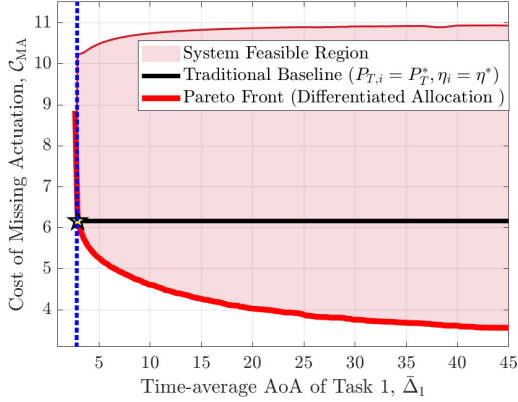


Fig. 4. Joint Optimization of time-average AoA of regular task and CoMA.

The goal of considering WNCS is to minimize the CoMA caused by data drops, while strictly guaranteeing the execution timeliness of the regular task. The Pareto frontier in the  $(P_{T,1}, P_{T,2}, \eta_1, \eta_2)$  decision space is presented in Fig. 4. The results reveal a significant trade-off between  $\Delta_1$  and  $C_{MA}$  when we employ differentiated resource allocation. Shifting toward the bottom-right of the frontier illustrates how the system trades off the AoA of regular tasks for improved critical-task reliability. Our proposed framework aims to identify the optimal trade-off point on the Pareto front based on varying system priorities. Furthermore, without task differentiation, CoMA and AoA of task 1 exhibit a positive correlation rather than a trade-off. Consequently, the traditional baseline is restricted to a horizontal line that indicates the optimal achievable CoMA. The star marks the minimum constraint threshold at which the baseline becomes feasible. The gap between the two curves demonstrates that employing differentiated allocation in WNCS can effectively guarantee the actuation reliability of critical information.

#### APPENDIX A SOLUTION OF MULTI-RATE GEO/GEO/C/C

Let  $n_1$  and  $n_2$  denote the number of active Task 1 and Task 2 instances, respectively. Under the constraint  $n_1 + Nn_2 \leq C$ , we partition the state space into levels based on  $n_1 \in \{0, 1, \dots, C\}$ . Let  $\mathcal{S}_{n_1}$  be the steady-state probability vector for Level  $n_1$ , forming the global vector  $\mathcal{S} = [\mathcal{S}_0, \mathcal{S}_1, \dots, \mathcal{S}_C]$ .

Since a maximum of one Task 1 can arrive per time slot, transitions to higher levels  $k > n_1$  are strictly bounded by  $k \leq n_1 + 1$ . This restricts the global generator matrix  $\mathbf{Q} = \mathbf{P} - \mathbf{I}$  to a Block Lower Hessenberg form. The global balance equation  $\mathbf{S}\mathbf{Q} = \mathbf{0}$  yields the level-wise equations for  $k \in \{1, 2, \dots, C\}$

$$\mathcal{S}_{k-1}\mathbf{Q}_{k-1,k} + \mathcal{S}_k\mathbf{Q}_{k,k} + \sum_{n_1=k+1}^C \mathcal{S}_{n_1}\mathbf{Q}_{n_1,k} = \mathbf{0}. \quad (20)$$

Using the matrix-geometric method, we assume there exist rate matrices  $R_k$  such that  $\mathcal{S}_{n_1} = \mathcal{S}_k \prod_{m=k+1}^{n_1} R_m$ ,  $\forall n_1 \geq k + 1$ . Substituting this relationship back into the level-wise equation and factoring out  $\mathcal{S}_k$  defines the matrix  $\tilde{Q}_k$

$$\tilde{Q}_k = \mathbf{Q}_{k,k} + \sum_{n_1=k+1}^C \left( \prod_{m=k+1}^{n_1} R_m \right) \mathbf{Q}_{n_1,k}. \quad (21)$$

This matrix  $\tilde{Q}_k$  models a censored Markov chain, effectively folding all excursion paths from higher levels directly into the local transition of level  $k$ . The (20) then elegantly simplifies to  $\mathcal{S}_{k-1}\mathbf{Q}_{k-1,k} + \mathcal{S}_k\tilde{Q}_k = \mathbf{0}$ , which explicitly defines the rate matrix

$$R_k = -\mathbf{Q}_{k-1,k}\tilde{Q}_k^{-1}, \quad (22)$$

with  $\mathcal{S}_k = \mathcal{S}_{k-1}R_k$ . This establishes a backward recursion initialized at  $k = C$  (where  $\tilde{Q}_C = \mathbf{Q}_{C,C}$ ) and proceeds downward to  $k = 1$ . Finally, the base vector  $\mathcal{S}_0$  is obtained by applying the geometric substitution to the boundary equation:

$$\mathcal{S}_0 \left[ \mathbf{Q}_{0,0} + \sum_{n_1=1}^C \left( \prod_{m=1}^{n_1} R_m \right) \mathbf{Q}_{n_1,0} \right] = \mathbf{0}, \quad (23)$$

alongside the normalization condition  $\sum_{n_1=0}^C \mathcal{S}_{n_1} \mathbf{1} = 1$ .

#### REFERENCES

- [1] S. Kaul, R. Yates, and M. Gruteser, "Real-time status: How often should one update?," in *Proc. IEEE INFOCOM, Orlando, FL, USA*, pp. 2731–2735, Mar. 2012.
- [2] R. D. Yates, Y. Sun, D. R. Brown, S. K. Kaul, E. Modiano, and S. Ulukus, "Age of information: An introduction and survey," *IEEE J. Sel. Areas in Commun.*, vol. 39, no. 5, pp. 1183–1210, Mar. 2021.
- [3] F. Zhao, N. Pappas, C. Ma, X. Sun, T. Q. S. Quek, and H. H. Yang, "Age-threshold slotted aloha for optimizing information freshness in mobile networks," *IEEE Trans. Wireless Commun.*, vol. 23, no. 11, pp. 17236–17251, Nov. 2024.
- [4] J. Luo, E. Delfani, M. Salimnejad, and N. Pappas, "From information freshness to semantics of information and goal-oriented communications," *ArXiv:2512.12758*, Dec. 2025.
- [5] A. Nikkhah, A. Ephremides, and N. Pappas, "Age of actuation and timeliness: Semantics in a wireless power transfer system," *IEEE Trans. Commun.*, vol. 74, pp. 4789–4804, Feb. 2026.
- [6] B. Li, J. Luo, T. Charalambous, and N. Pappas, "Model predictive communication for timely status updates in low-altitude networks," *ArXiv:2604.20610*, Apr. 2026.
- [7] X. Qiu, C. Fu, S. Sun, Y. Du, V. Chau, W. Wu, J. Luo, and S. Han, "Minimizing age of result in multi-task networked control systems," *IEEE J. Sel. Areas in Commun.*, vol. 43, no. 9, pp. 3150–3166, Sept. 2025.
- [8] F. Zhao, N. Pappas, M. Zhang, and H. H. Yang, "Age of information in random access networks with energy harvesting," *IEEE J. Sel. Areas in Commun.*, vol. 43, no. 11, pp. 3813–3829, Nov. 2025.
- [9] I. D. Moscholios and M. D. Logothetis, "The erlang multirate loss model," in *Efficient Multirate Teletraffic Loss Models Beyond Erlang*, pp. 3–64, Wiley, Feb. 2019.